# Membrane Current Responses
# of Skate Photoreceptors

M. Carter Cornwall, Harris Ripps, Richard L. Chappell, and
Gregor J. Jones

From the Department of Physiology, Boston University School of Medicine, Boston, Massa-
chusetts 02118; the Eye Research Institute and Department of Ophthalmology, University
of Illinois College of Medicine, Chicago, Illinois 60612; the Department of Biological
Sciences, Hunter College and the City University of New York Graduate Center, New York
10021; and the Marine Biological Laboratory, Woods Hole, Massachusetts 02543

ABSTRACT   Light-evoked membrane currents were recorded with suction elec-
trodes from the outer segments of individual photoreceptors enzymatically disso-
ciated from the skate retina. The intensity-response relation of dark-adapted cells
closely followed a Michaelis function for which a half-saturating response was elic-
ited by a flash intensity that produced about 36 photoisomerizations. Dim-light
responses, as well as the early rising phase of the responses to a wide range of flash
intensities, could be described by a reaction scheme that involved a series of four
first-order delay stages. The number of delay stages required to model the rising
phase of the photocurrents did not change in light adaptation. However, back-
ground illumination that reduced sensitivity by 1.5 log units, or a bleaching expo-
sure that resulted in a nearly equivalent desensitization, shortened significantly the
time scale of the responses. In both instances there were two- to threefold
increases in the rate constants of the transitional delays, and almost complete sup-
pression of the tail current that characterized the response of the dark-adapted
cell. These findings suggest that although light adaptation alters the gain and
kinetics of the transduction mechanism, the nature of the intervening processes is
the same in dark- and light-adapted photoreceptors. Moreover, the results show
clearly that there is no need to postulate the existence of a second class of cone-
like rods to account for the remarkable ability of skate photoreceptors to respond
to incremental stimuli presented on "saturating" background fields or after expo-
sure to an intense bleaching light.

## INTRODUCTION

There is good evidence that in some species of skate (*Raja erinacea* and *R. oscellata*),
vision is mediated solely by rods, the visual cells that give rise to nocturnal vision in
the duplex (rod-cone) retinae of other vertebrates. The photoreceptors have a uni-
form, rod-like appearance (Dowling and Ripps, 1970; Szamier and Ripps, 1983), the

aspartate-isolated receptor potential of the dark-adapted retina exhibits the high sensitivity characteristic of rod-mediated vision (Dowling and Ripps, 1972; Green et al., 1975), and only one vitamin $A_1$-based photopigment (rhodopsin) has been detected by reflection densitometry (Dowling and Ripps, 1970) and transmission spectrophotometry (Brin and Ripps, 1977).

But unlike the situation in other vertebrates, the rod mechanism in skate is able to resolve rapidly flickering light (Green and Siegel, 1975), and is capable of responding to incremental stimuli in the presence of intense background illumination that should thoroughly saturate the rod photocurrent (Dowling and Ripps, 1970, 1971, 1972, 1977). These cone-like properties have created a lingering doubt as to whether there exist in the skate retina two classes of visual cells that are morphologically and photochemically indistinguishable, but which behave functionally like the rods and cones of mixed retinae. Conversely, if a single cell type is subserving vision in this elasmobranch, it would be of interest to examine its unusual response properties under conditions that remove the influence of inter-receptor coupling or feedback from second-order cells. Both of these issues have been addressed in the present study, in which we have recorded with suction electrodes the photocurrent of solitary photoreceptors under dark- and light-adapted conditions.

## MATERIALS AND METHODS

Skates (*R. erinacea* and *R. oscellata*) were netted in the deep waters of Vineyard Sound and maintained in cold, aerated seawater tanks. After at least 2 h in complete darkness an animal was anesthetized (0.1% 3-aminobenzoic acid ethyl ester, tricaine, MS 222) and pithed, and the eyes were removed under dim red light. All subsequent manipulations were performed under deep red or infrared illumination with the aid of an IR-sensitive image converter. The globe was sectioned equatorially, the posterior segment was drained of vitreous, and the retina was separated from the eyecup and transferred to a plastic centrifuge tube containing 0.2 ml (163 units) papain (3125; Sigma Chemical Co., St. Louis, MO) preactivated with 3 mg cysteine in 5 ml of a modified culture medium (Leibowitz L-15; GIBCO Laboratories, Grand Island, NY). To maintain normal osmolarity, the L-15 was supplemented with 102 mM NaCl, 350 mM urea, 5.5 mM glucose and adjusted to pH 7.7–7.8 with concentrated NaOH. After 45 min incubation, the tissue was washed twice (2 × 5 min) in 15 ml of the enzyme-free medium, drained of fluid, and immersed in 3 ml of the modified L-15. The retinas were then disrupted by repeated passage (20 ×) through the flame-polished tip of a Pasteur pipette. Clumps of retinal tissue settled to the bottom of the tube (for later trituration if needed), leaving large numbers of isolated photoreceptors and small clusters of visual cells as the predominant constituents of the supernatant.

An aliquot of the suspension was placed on a glass coverslip mounted on the stage of an inverted microscope that was housed in a light-tight, electrically shielded enclosure. An open-sided fluid-filled chamber was formed between the coverslip and the cone of a 10× water immersion objective that served as the final element of a dual-beam photostimulator (cf. Cornwall et al., 1983). The optical system provided test and adapting fields that could be controlled independently with respect to intensity, duration, and spectral composition. For this study, the stimulus fields illuminated uniformly the area viewed by a 40× microscope objective that imaged the specimen field onto the screen of an IR-sensitive video system. Photometry with the aid of a calibrated photometer (model 80X; United Detector Technology, Hawthorne, CA) at the plane of the preparation indicated that the photon flux delivered

by the unattenuated "monochromatic" ($\lambda_{max}$ = 500 nm) test beam was 7.49 × $10^6$ photons $\mu m^{-2}$ $s^{-1}$; that of the background (or bleaching) beam ($\lambda_{max}$ = 560 nm) was 1.92 × $10^7$ photons $\mu m^{-2}$ $s^{-1}$. The interference filters in the two chromatic beams had half-bandwidths of ~10 nm.

The outer segment of an intact photoreceptor (either single or from amongst a small cluster) was drawn into the tip of a glass micropipette that had been shaped and fire-polished to fit snugly around the cell membrane. The pipette was filled with an elasmobranch Ringer solution (Lasater et al., 1984) that was also used to superfuse the exposed rod inner segment during an experimental run. The solution in the barrel of the pipette was in electrical contact via a Ag/AgCl pellet with the input stage of a current-to-voltage converter (EPC-7; List-Electronic, Darmstadt, FRG), the output of which was amplified, displayed on an ink-writing oscillograph (Gould Inc., Cleveland, OH), and recorded on an FM tape recorder (Racal Recorders Ltd., Hythe, England). The return of the virtual ground configuration was connected to the superfusion chamber by a Ringer-filled agar bridge through a second Ag/AgCl pellet. For analysis, the responses were replayed through an active low-pass filter (8-pole Bessel; Frequency Devices Inc., Haverhill, MA), and digitized using the software package ASYSTANT+ (Asyst Software Technologies Inc., Rochester, NY).

## RESULTS

### Isolated Photoreceptors

The micrographs of Fig. 1 show examples of the two cellular configurations from which current recordings were obtained. Responses from an individual cell within a cluster (*top*) did not differ in any obvious way from those obtained in recordings from the dissociated cell (*bottom*). The dimensions of the outer segments of isolated photoreceptors ($n$ = 92) did not vary by more than 0.4 $\mu m$ from the mean values of 3.41 $\mu m$ diameter, 28.7 $\mu m$ length.

### Current Responses of Dark-adapted Cells

Fig. 2 *A* shows current recordings from the outer segment of a skate rod in response to a series of 220-ms flashes of monochromatic light ($\lambda_{max}$ = 500 nm) that extend over an intensity range of 1.94 photons $\mu m^{-2}$ to 1.64 × $10^4$ photons $\mu m^{-2}$. In each instance, upward deflections represent a decrease in the cell's dark current; i.e., the closure of light-activated channels in the outer segment membrane. Although response kinetics will be considered later (see Fig. 3), it is apparent that the time to peak decreased with increasing intensity, and that beyond response saturation ($I$ > 200 photons $\mu m^{-2}$) the duration of the current plateau increased as the intensity increased. For this cell, the maximum light-evoked current ($R_{max}$) was 19.5 pA, and the flash intensity ($\sigma$) required to elicit a half-maximal response was ~14.7 photons $\mu m^{-2}$.

Complete intensity-response functions were derived from current recordings obtained on 26 dark-adapted rods. The mean values of $R_{max}$ and $\sigma$ were 12.39 pA (±0.61 SEM) and 9.20 photons $\mu m^{-2}$ (±0.94 SEM), respectively. As noted in earlier reports (cf. Baylor et al., 1979*b*), the variability in these parameters is attributable in part to variations in the length of the outer segment drawn into the suction electrode, and in part to differences in the seal resistance between electrode and cell membrane. The results, shown graphically in Fig. 2 *B*, indicate that the averaged
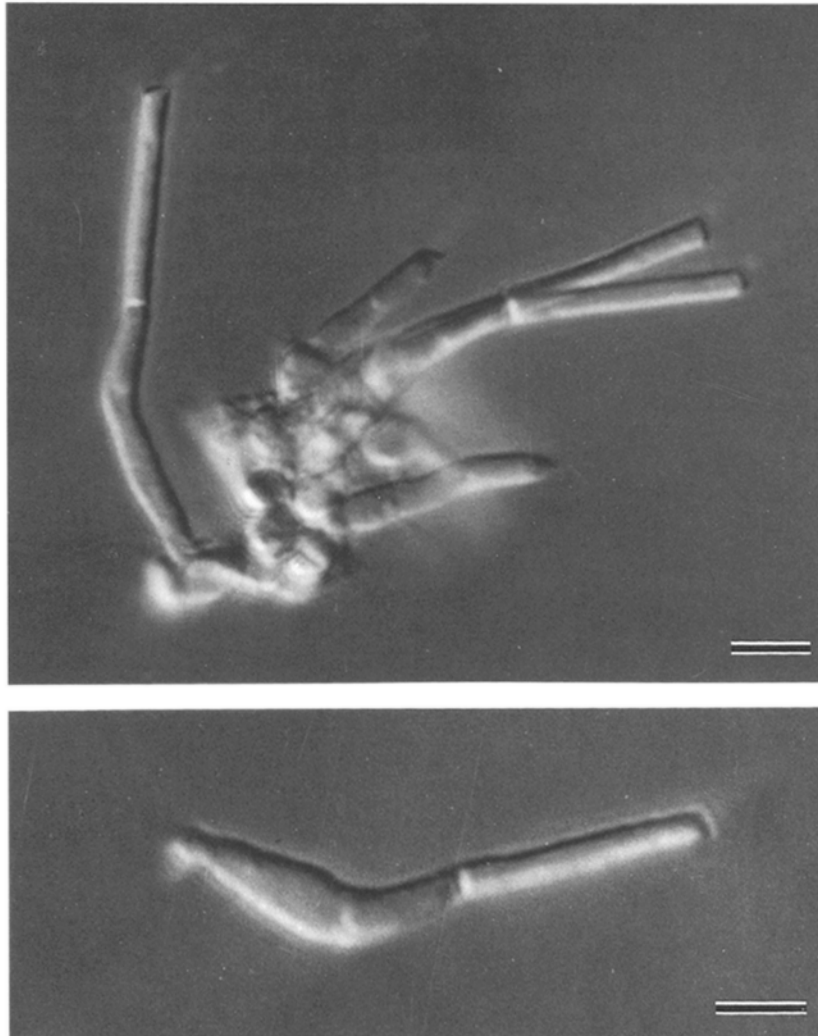
FIGURE 1.   Photomicrographs of enzymatically isolated skate rods. (Top) A cluster of photo-receptor cells. (Bottom) A single isolated cell. Bars, 10 $\mu$m.

data, normalized with respect to $R_{max}$ and $\sigma$, are described well by an equation of the form:

$$R = R_{max} [I^n/(I^n + \sigma^n)],  \tag{1}$$

where $R$ is the peak current (pA) elicited by a flash of intensity $I$ (photons $\mu m^{-2}$), and $n$ is a constant. Using the nonlinear curve-fitting routine of ASYSTANT+ to generate a least-squares fit through the data (continuous line) gave a value for $n$ of 1.07; i.e., the curve closely approximates a Michaelis function for which $n = 1$.

## Response Kinetics of Dark-adapted Rods

In toad rods (Baylor et al., 1979a, 1980; Matthews, 1983) the kinetics of the light response can be modeled by a series of reactions that incorporate four first-order delays, i.e., four linear stages (with appropriate rate constants) in the transduction process. A similar number of stages appear to be involved in shaping the membrane current of skate rods in response to dim-light flashes. Fig. 3 shows the temporal course of the light-evoked current (average of responses from 21 cells) produced by photic stimuli in the lower (linear) region of the intensity-response function. The curves drawn through the data represent the Poisson and Independent Activation
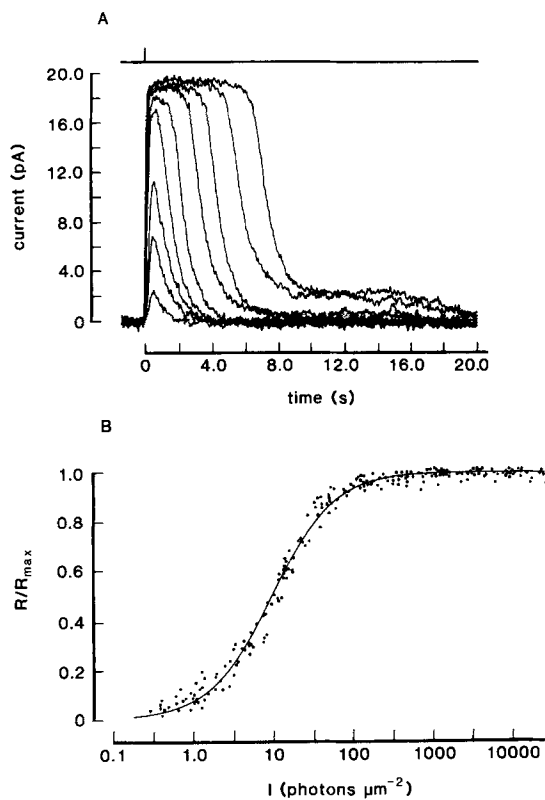


FIGURE 2. Responses of dark-adapted skate rods. (A) Superimposed traces of photocurrents recorded from the outer segment of a dark-adapted rod in response to 220-ms light flashes (stimulus marker shown on upper trace). The light intensity was increased from 1.94 photons $\mu m^{-2}$ to $1.64 \times 10^4$ photons $\mu m^{-2}$ in steps of ~0.5 log units. (B) Normalized intensity-response function from 26 cells. The peak amplitudes recorded with different flash intensities were normalized with respect to the maximum response of each cell, and the data were positioned on the scale of abscissae by sliding each intensity-response function laterally to coincide at the mean value of $\sigma$, the light intensity producing a half-maximal response. The curve is a least-squares fit to Eq. 1.

expressions of Baylor et al. (1979a) and Matthews (1983), modified to describe the response to a 220-ms light pulse. Thus for a light pulse of finite duration ($\Delta t$):

$$R(t) = \rho(t) - \rho(t - \Delta t); \ \rho(t < 0) = 0,$$                                        (2)

where $R(t)$ is the photocurrent at time $t$ after the onset of the stimulus and $\rho(t)$ is the response to a light step ($\Delta t$ approaches infinity) for the two models described by Fuortes and Hodgkin (1964, Eq. 10) and by Baylor et al. (1974, Eq. 40), i.e.:

$$\text{(Poisson)} \qquad \rho(t) = k(I_F/\alpha)\{1 - e^{-\alpha t} \sum_{r=0}^{n-1} [(\alpha t)^r]/r!\}$$                (3)

$$(\text{Ind. Act.}) \qquad \rho(t) = k(I_F/\alpha)(1 - e^{-\alpha t})^n \tag{4}$$

where $I_F$ is the flux density of the incident light (photons $\mu m^{-2}s^{-1}$), $k$ is a proportionality constant that relates light intensity (through quantal absorption) to photocurrent, and $n$ is the number of low-pass filters with equivalent rate constants $\alpha$ (Poisson). In the case of Independent Activation, the rate constants for a series of $n$ filters is $n\alpha$, $(n - 1)\alpha$, . . . $\alpha$. For skate rods, the Independent Activation scheme with four stages of delay and $\alpha = 2.26$ s$^{-1}$ provided the best fit to the low-intensity flash data.

An alternative method for estimating the value of $n$ (Baylor et al., 1979a; Matthews, 1983) also revealed that the shape of the light response can be approximated by a series of four delay stages. A double-logarithmic plot of $(R/I)$ against time after flash onset enables one to examine the kinetics of the early, presumably linear portion of the responses to brighter flashes. Because the rising phase of the responses occurs during the light pulse (i.e., analogous to a step of light), the number of delay
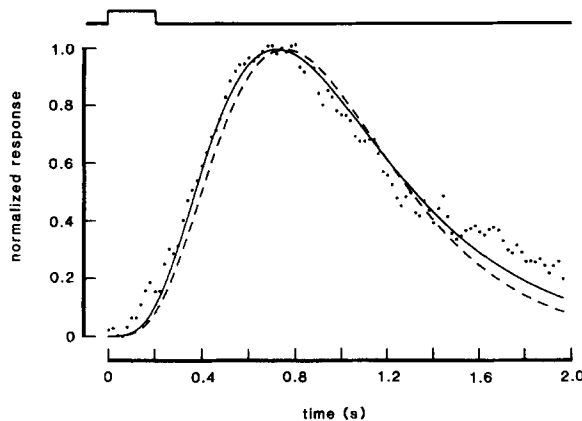


FIGURE 3. Membrane current response of dark-adapted skate rods to dim-light flashes. The points show the time course of the normalized average of 21 responses to 220-ms dim-light flashes (*upper trace*). The continuous line is a least-squares minimization of the data to Eq. 2 for Independent Activation with $n$ set at four stages, and a rate constant of 2.26 s$^{-1}$. The dashed line is a fit of the Poisson model of equation 2, also with four stages; the rate constant is 4.61 s$^{-1}$.

stages is obtained from the slope of the steeply rising portion of the curve. Fig. 4 shows the results of such a plot for the responses of Fig. 2 A. The filled circles are a plot of Eq. 2 for independent activation with $\alpha = 2.60$ s$^{-1}$ and $n = 4$. Comparable results were obtained with four other rods on which kinetic analyses were performed.

### Responses of Light-adapted Cells

Fig. 5 A shows current responses to 220-ms light pulses of increasing intensity recorded first in darkness, and then 21 min after the onset of a background light ($\lambda = 560$ nm) that delivered $1.03 \times 10^3$ photons $\mu m^{-2}$ s$^{-1}$. The responses of the dark-adapted cell, like those shown earlier (Fig. 2), rapidly increase in amplitude as the flash intensity is increased, and reach a peak (i.e., saturate) at an intensity of ~200 photons $\mu m^{-2}$; with higher intensities, the plateau of the saturating response is

prolonged, and the recovery of the dark current is delayed further by a slowly decaying "tail" current.

Exposure to the background field at first saturated the photocurrent, and the cell remained entirely unresponsive to incremental stimuli for almost 2 min. However, after 21 min of exposure to the luminous field (at which time the light-evoked currents had stabilized), $R_{max}$ grew to about half of its dark-adapted value. Due to electronic drift and small fluctuations in the position of the suction electrode with respect to the outer segment, it was not possible to monitor accurately the changes in radial current that take place during so long an exposure. Nevertheless, it is obvious that a significant decrease in the sustained receptor current must occur to allow for the release from saturation, the partial return of the light-suppressible current, and the gradual increase in $R_{max}$.
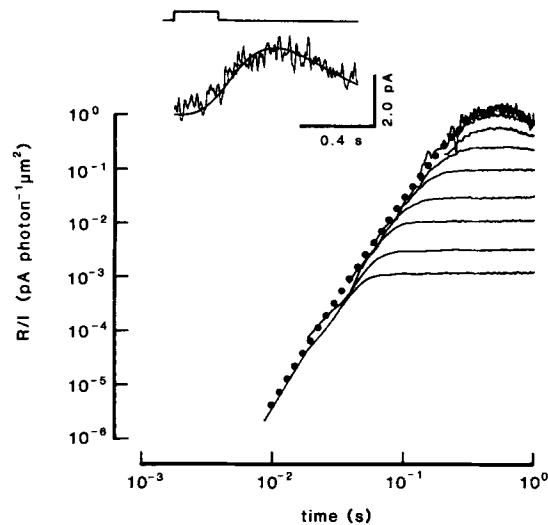


FIGURE 4. Analysis of the linearity with light intensity of the early rising phases of responses to bright lights. The membrane current responses of Fig. 2 A are replotted on double logarithmic coordinates after dividing the responses by the incident light intensity. Note that due to noise in the recordings at earlier times, the curves corresponding to lower stimulus intensities start later than those for higher intensities. Inset shows the smallest response on a linear scale with a smooth curve according to Eq. 2 for the Independent Activation model with four stages and fitted rate constant of 3.28 s$^{-1}$. Filled circles on the log/log plot are the same curve after dividing by the appropriate light flux. Both the response in the linear region and the early rising phases of responses to brighter lights fit the model with four stages; i.e., the limiting slope of the line described by the circles is four.

In addition to the reduction in $R_{max}$ (response compression), there was also a change in the waveform of the photocurrent. Even relatively intense flashes did not evoke responses having a broad plateau, nor did the falling phase exhibit a prominent tail current. None of these changes can be attributed to the effects of bleached rhodopsin; after 20 min of continuous exposure, the background had photoisomerized <0.5% of the rhodopsin content of the visual cell.

Somewhat comparable results were obtained (Fig. 5 B) when a light-adapted state was induced by a brief (9 s) exposure to a bright background field that bleached a significant fraction of the visual pigment (cf. Pepperberg et al., 1978). In this experiment, the flux density of the bleaching beam (1.83 × 10$^6$ photons $\mu$m$^{-2}$ s$^{-1}$) was

THE JOURNAL OF GENERAL PHYSIOLOGY · VOLUME 94 · 1989

chosen, based on preliminary data, to produce a desensitization ($\Delta\sigma$) similar to that induced by the continuous background. Taking into account the collecting area of the visual cell (cf. Baylor et al., 1979b), the number of photoisomerizations ($P^*$) is given by the expression:

$$P^* = (I_F t)2.303 D_\lambda V_{\lambda'} \pi r^2 l \gamma \phi \tag{5}$$

where $I_F$ is the radiant flux density (photons $\mu m^{-2} s^{-1}$) delivered for time $t$, $D_\lambda$ =
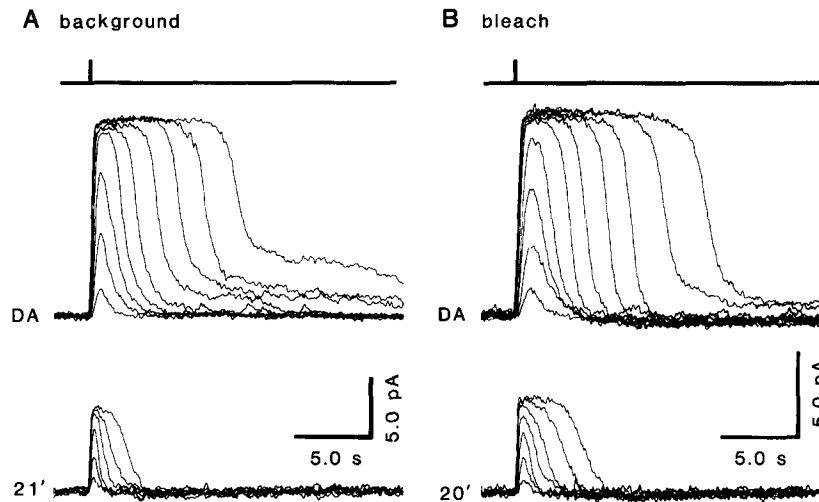


FIGURE 5.  Membrane current responses before (DA, dark-adapted), and after adaptation to a background light or after exposure to a bleaching light that produced approximately equivalent desensitizations. For each part of the figure, the traces are superimposed recordings of photocurrents elicited by 220-ms light flashes, with intensities increasing in steps of ~0.5 log unit. (A) Background adaptation. The light flashes for the dark-adapted cell increased from $0.19 \times 10^1$ to $1.64 \times 10^4$ photons $\mu m^{-2}$. The lower recordings were made 21 min after the onset of a background light of intensity $1.03 \times 10^3$ photons $\mu m^{-2} s^{-1}$; the incremental test flashes increased from $6.86 \times 10^1$ to $1.64 \times 10^4$ photons $\mu m^{-2}$. (B) Bleaching adaptation, from a different cell. The light flashes for the dark-adapted cell increased from $6.4 \times 10^{-1}$ to $1.64 \times 10^4$ photons $\mu m^{-2}$. The lower recordings were obtained 20 min after a 9-s exposure to 560-nm light that bleached 4–5% of the rhodopsin content of the cell. The responses are to test flashes that increased from $6.86 \times 10^1$ to $1.64 \times 10^4$ photons $\mu m^{-2}$.

$0.016 \ \mu m^{-1}$ is the specific transverse pigment density at $\lambda_{max}$ of the rhodopsin absorbance spectrum (Harosi, 1975), $V_{\lambda'} = 0.31$ is the efficacy of light at wavelength $\lambda'$ (560 nm) relative to that at $\lambda_{max}$ (500 nm), $r$ and $l$ are the radius (1.7 $\mu m$) and length (28.7 $\mu m$) of the rod outer segment, $\gamma = 0.67$ is the efficiency of isomerization for absorbed quanta (Dartnall, 1957), the factor $\phi = 0.6$ is an approximate correction for the use of unpolarized light incident at right angles to the long axis of the photoreceptor, and 2.303 transforms natural to common logarithms in converting absorbance ($D$) to absorptance.

Based on Eq. 5, $P^* = 1.98 \times 10^7$ represents the number of rhodopsin molecules

isomerized during the 9-s exposure. If the population density of rhodopsin molecules in the disc membranes of a receptor outer segment (ROS) in skate is similar to that seen in other species, i.e., $\sim$28,000 $\mu m^{-2}$ (Roof and Heuser, 1982; Liebman et al., 1987), then the nearly 2,000 disc membranes of a skate ROS would contain about $5 \times 10^8$ molecules of rhodopsin, $\sim$4.1% of which were bleached in the course of the 9-s exposure. Estimates based on the effective molar concentration of rhodopsin in situ (2.7 mM) gives a value of 4.7%, whereas considering the fraction bleached to be given by the expression $c_b/c_o = 1 - \exp(-k\alpha\gamma I_F t)$, where $c_o$ and $c_b$ are the concentrations of rhodopsin before and after bleaching, respectively, $k$ is the product of $V_{\lambda'}$ and a correction factor for dichroism, and $\alpha$ is the in situ extinction coefficient of rhodopsin ($1.56 \times 10^{-16}$ cm$^2$/chromophore), yields a value of 4.4%. In any event, immediately after the bleaching exposure there was again a period of $\sim$3 min during which the cell was entirely unresponsive to photic stimulation, but in darkness the cell gradually regained its ability to respond to test flashes. After the responses had stabilized (lower traces of Fig. 5 $B$), there was clearly a significant degree of response compression (i.e., the maximum photocurrent was less than half of its prebleach [DA] value), and response kinetics resembled that seen in the presence of a luminous background.

Fig. 6 compares intensity-response data obtained in the course of the background and bleach experiments shown in Fig. 5. For the earlier times during the two experimental runs, the amplitudes of the current responses were changing rapidly as the cells light adapted. Accordingly, the times indicated represent only the start of the intensity series, and none of the curves are comparable to the intensity-response functions obtained under steady-state conditions, i.e., after 21 min in the presence of the background field, or after 20 min in darkness after the bleaching exposure. Using the value of $\sigma$ as an index of sensitivity, it is apparent that the changes in sensitivity ($\Delta\sigma$) that were reached ultimately were comparable; i.e., 1.47 log units with background adaptation, and 1.51 log units after the bleach. Thus, nearly equivalent losses in sensitivity occurred in the presence of weak background illumination that initially saturated the photocurrent (Fig. 6 $A$), or in darkness after a photic exposure that bleached $\sim$4–5% of the rhodopsin content of the visual cell (Fig. 6 $B$). Moreover, when plotted as $R/R_{max}$ (not shown but see legend to Fig. 6) each final data set is adequately described by Eq. 1 with $n$ of $\sim$1; i.e., of the form shown in Fig. 2 $B$.

### Kinetics of the Light-adapted Cell

The double logarithmic plots of Fig. 7 provide a comparison between the kinetic parameters of dark-adapted cells with those that result from background (Fig. 7 $A$) and bleaching (Fig. 7 $B$) adaptation. The data, taken from the recordings of Fig. 5, show the sensitivities of responses to a series of test flashes given both in darkness and after the photoreceptor had stabilized to the prevailing level of light adaptation. It is particularly noteworthy that in all cases, the function plotted according to the Independent Activation model (cf. Eqs. 2 and 4) for $n = 4$ describes well the shape of the responses to low-intensity flashes (see insets), and provides a good fit to the rising phase of all the current responses. Thus, there appears to be no change in the

number of low-pass filter stages required to model the photocurrents of light- and dark-adapted receptors.

Baylor et al. (1979a) showed that background illumination accelerated the current responses of toad rod outer segments to dim incremental stimuli. The inset of Fig. 7 shows that in skate both background and bleaching adaptation produced a significant reduction in the time-to-peak ($t_{peak}$) of the threshold responses to dim-light flashes. In the case of the background, $t_{peak}$ fell from 0.61 to 0.29 s (a drop of
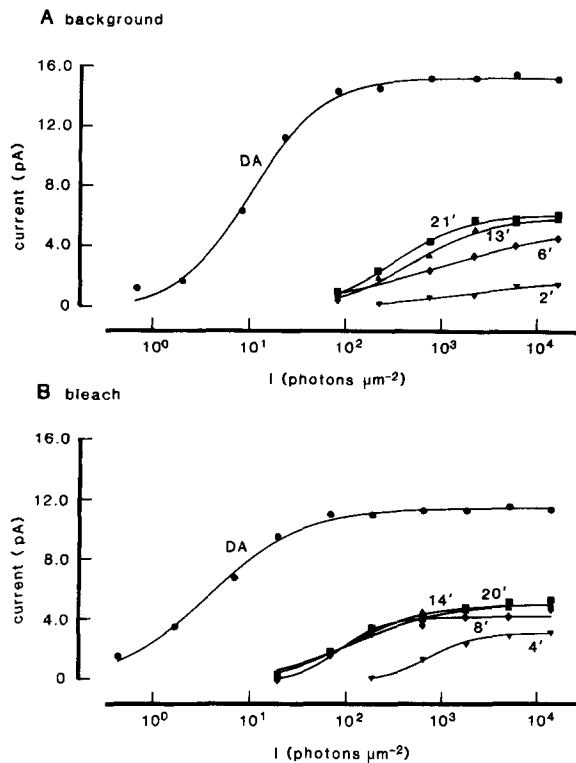


FIGURE 6. Changes in the relationship between peak response amplitude and light intensity during background adaptation and after pigment bleaching. The data points are peak amplitudes of membrane current responses to 220-ms flashes plotted against the logarithm of the light intensity. Data obtained from the same two cells illustrated in Fig. 5. In both panels, the data points have been fitted by least-squares minimization to Eq. 1. For the responses in steady-state, the curve fits were constrained to have the same value of the exponent $n$ in this equation as that for the best fit for the dark-adapted cell. (A) Background adaptation. The times indicated are with reference to the onset of the background light (see text for details). At 21 min, the cell had reached a steady state, and the change in sensitivity ($\Delta\sigma$) was +1.47 log units; the value of $n$ was 1.13. (B) Bleaching adaptation for the conditions given in the legend to Fig. 5. The times indicated are times after the 9-s bleaching exposure. At 20 min, when the responses indicated that the cell had reached a steady state, the change in sensitivity ($\Delta\sigma$) was +1.51 log units; the value of $n$ was 0.90.

53%); after the bleach, $t_{peak}$ fell from 0.77 to 0.43 s (a reduction of 44%). Moreover, both forms of light adaptation produced marked increases in the rate constants of the linear portion of the responses to brighter flashes: 2.7-fold with the background field, and 2.1-fold as a result of the bleach (see legend to Fig. 7). Intracellular recordings from toad rods (Leibovic et al., 1987) also show that background adaptation exerts a greater effect on response kinetics than a bleaching exposure that produces an equivalent loss of sensitivity.

The Effects of Large Bleaches

The results of Figs. 5 A and 6 A indicate how effectively the skate photoreceptor can adapt to a continuously illuminated field that initially saturates the photocurrent; i.e., with time, the cell regains its ability to respond to incremental stimuli. In fact, the same phenomenon can be demonstrated with background fields 100× more
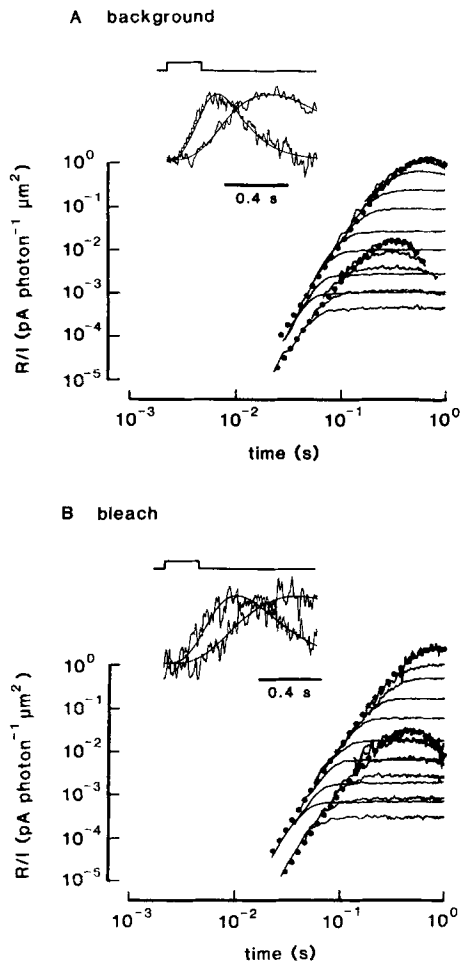


FIGURE 7. Analysis of the linearity with light intensity of the early rising phases of responses to bright lights before and after background adaptation and before and after bleaching adaptation. The membrane current responses of Fig. 5 are replotted on double logarithmic coordinates after dividing the responses by the incident light intensity. Insets show the smallest responses on a linear scale after normalization to the peak value; the smooth curves are drawn according to Eq. 2 for the Independent Activation model with four stages. The filled circles on the log/log plots are the same curves before normalization and after dividing by the appripriate light flux. (A) Background adaptation. The slower response in the inset was for the dark-adapted cell, having a peak amplitude of 2.2 pA, and a fitted rate constant of 2.49 s$^{-1}$. The faster response was for the light-adapted cell: peak amplitude 2.8 pA, and the fitted rate constant was 6.76 s$^{-1}$. (B) Bleaching adaptation. The slower response in the inset was for the dark-adapted cell, with a peak amplitude of 1.9 pA, and a rate constant of 1.86 s$^{-1}$. The faster response was for the light-adapted cell: peak amplitude 2.1 pA, and the fitted rate constant was 3.97 s$^{-1}$.

intense (not shown), although the time required for the cell to become responsive is then greatly prolonged (>30 min), and $\sigma$ is shifted far to the right on the scale of abscissae (cf. Dowling and Ripps, 1972). Very similar changes in time course and sensitivity were seen when light adaptation was induced by a 30-s photic exposure, calculated to bleach ~86% of the rhodopsin content of the photoreceptor. As

shown in the upper recording of Fig. 8 A, the initial exposure had a profound effect on the response; only after ~40 min in darkness was the cell again responsive to test stimuli. However, another 30-s full intensity exposure delivered after 96 min of "dark adaptation," evoked a vigorous (but smaller) response from which the cell recovered in <30 s despite the fact that no pigment regeneration had occurred after either bleach. With ~98% of the available rhodopsin bleached, the same stimulus,
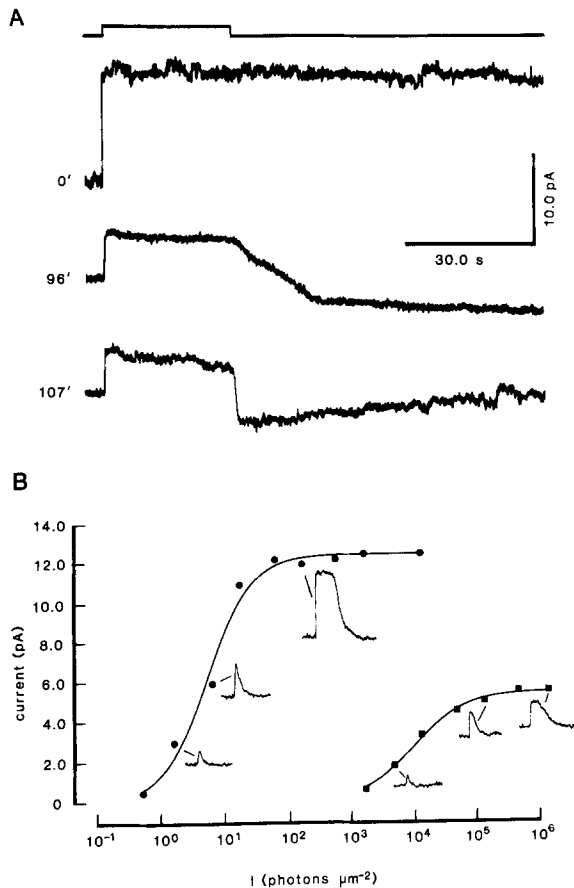


FIGURE 8. Effects of intense bleaching light. (A) Photocurrents elicited by 30-s steps of unattenuated light (500 nm) from the test beam, first in a dark-adapted cell (top trace), then 96 min after the initial exposure (middle trace), and finally, after an additional 11 min of darkness (bottom trace, 107 min after the initial 30-s bleach). The time course of the light stimulus is indicated above the traces. (B) Response-intensity functions of the cell shown in A, taken first in the dark-adapted state (filled circles), and again after 93 min in darkness following the initial 30-s bleach (filled squares). The smooth curves through the filled circles (left) and filled squares (right) were drawn according to Eq. 1 where $R_{max}$ = 12.5 pA, $\sigma$ = 6.6 photons $\mu m^{-2}$, and $n$ = 1.2; and $R_{max}$ = 5.5 pA, $\sigma$ = 1.0 × $10^4$ photons $\mu m^{-2}$, and $n$ = 1.1, respectively. Responses shown beside these curves are representative of data from which the curves were constructed.

given 10 min later (trace at 107 min), evoked a response that was 40% of the maximum photocurrent recorded from the dark-adapted cell. Moreover, there was almost no post-stimulus desensitization; i.e., the current rebounded beyond its newly established dark level at light offset.

Fig. 8 B shows intensity-response data to 220-ms flashes obtained from the dark-

adapted cell, and then 96 min after the initial bleaching exposure. The two sets of data are described well by the same Michaelis function, although there is clearly a significant degree of response compression, $(V_{max})_d = 12.7$ pA, $(V_{max})_b = 5.1$ pA, and a shift in $\sigma$ of >3 log units.

## DISCUSSION

The results of this study demonstrate that a single class of photoreceptor in skate displays the full complement of adaptive properties reported earlier for the aspartate-isolated receptor potential (Dowling and Ripps, 1972) as well as for the responses of second- and third-order retinal neurons (Dowling and Ripps, 1970, 1971, 1977; Green et al., 1975; Naka et al., 1988). Thus, there is no need to invoke hypotheses involving feedback mechanisms, receptor coupling, or two classes of visual cell to account for the remarkable range of intensities over which the skate visual system operates.

At the low end of this range, the dark-adapted photoreceptor is a supremely sensitive photon detector (Hecht et al., 1942). For 500 nm light, a half-saturating response is elicited by a flash intensity of 9.19 photons $\mu m^{-2}$ (Fig. 2 $B$). Inserting this value for $I_F \cdot t$, and $V_{500} = 1$ in Eq. 5 indicates that $\sigma$ corresponds to ~36 photoisomerizations, a value that falls within the range of sensitivities (20–60 photoisomerizations) reported for red and green rods of the toad (cf. Matthews, 1983) as well as for rods of the cynomolgous monkey (Baylor et al., 1984). Also noteworthy is the observation that light-evoked responses of ~1 pA were detectable with stimuli 1.5 log units less intense, i.e., corresponding to single isomerizations. These dim-flash responses had peak times of ~0.8 s at 21°C, comparable to that of rods from other cold-blooded vertebrates (Baylor et al., 1983; Lamb, 1984).

The kinetics of the light-suppressible currents provide additional insight into the response properties of skate visual cells. In the dark-adapted state, the responses to weak flashes are described well by equations derived by Baylor et al. (1974) to estimate the number and rate constants of the hypothetical delay stages intervening between quantal absorption and the closure of membrane channels mediating the receptor's dark current. Based on their scheme for independent activation, the mean values of $n = 4$ and $\alpha = 2.26$ s$^{-1}$ we obtain for skate are in good agreement with results reported in previous studies of toad rods (Baylor et al., 1980; Matthews, 1983).

Interestingly, the number of delay stages required to shape the rising phase of the photocurrents did not change in light adaptation, regardless of whether the adaptation was induced by a background field that reduced sensitivity by 1.5 log units, or by a bleaching exposure that resulted in a nearly equivalent sensitivity loss. In both instances there were two- to threefold increases in the rate constants of the transitional delays, a pronounced shortening of the time-to-peak of the response, and almost complete suppression of the prolonged tail current that characterized the responses of the dark-adapted cell. The sharpening of the response waveform in light adaptation helps to explain the ability of skate photoreceptors to resolve rapidly flickering light at high intensities (Green and Siegel, 1975).

Despite the marked changes in response kinetics with light adaptation, stimulus-

response functions, obtained when the responses had stabilized to prevailing conditions, were similar in form to that of the dark-adapted preparation; i.e., described by Eq. 1 in which $n = 1$ (Michaelis). This observation, and the fact that the number of delay stages remains unchanged, suggests that although light adaptation modifies the gain and kinetics of the transduction mechanism, the same processes are involved in regulating sensitivity and time course within the outer segments of dark- and light-adapted cells (cf. Baylor et al., 1980).

REFERENCES

Baylor, D. A., A. L. Hodgkin, and T. D. Lamb. 1974. The electrical response of turtle cones to flashes and steps of light. *Journal of Physiology.* 242:685–727.

Baylor, D. A., T. D. Lamb, and K.-W. Yau. 1979a. The membrane current of single rod outer segments. *Journal of Physiology.* 288:589–611.

Baylor, D. A., T. D. Lamb, and K.-W. Yau. 1979b. Responses of retinal rods to single photons. *Journal of Physiology.* 288:613–634.

Baylor, D. A., G. Matthews, and K.-W. Yau. 1980. Two components of electrical dark noise in toad retinal rod outer segments. *Journal of Physiology.* 309:591–621.

Baylor, D. A., G. Matthews, and K.-W. Yau. 1983. Temperature effects on the membrane current of retinal rods of the toad. *Journal of Physiology.* 337:723–734.

Baylor, D. A., B. J. Nunn, and J. L. Schnapf. 1984. The photocurrent, noise and spectral sensitivity of rods of the monkey *Macaca fascicularis. Journal of Physiology.* 357:575–607.

Brin, K. P., and H. Ripps. 1977. Rhodopsin photoproducts and rod sensitivity in the skate retina. *Journal of General Physiology.* 69:97–120.

Cornwall, M. C., A. Fein, and E. F. MacNichol, Jr. 1983. Spatial localization of bleaching adaptation in isolated vertebrate rod photoreceptors. *Proceedings of the National Academy of Sciences.* 80:2785–2788.

Dartnall, H. J. A. 1957. The Visual Pigments. Methuen, London. 216 pp.

Dowling, J. E., and H. Ripps. 1970. Visual adaptation in the retina of the skate. *Journal of General Physiology.* 56:491–520.

Dowling, J. E., and H. Ripps. 1971. S-potentials in the skate retina. Intracellular recordings during light and dark adaptation. *Journal of General Physiology.* 58:163–189.

Dowling, J. E., and H. Ripps. 1972. Adaptation in skate photoreceptors. *Journal of General Physiology.* 60:698–719.

Dowling, J. E., and H. Ripps. 1977. The proximal negative response and visual adaptation in the skate retina. *Journal of General Physiology.* 69:57–74.

Fuortes, M. G. F., and A. L. Hodgkin. 1964. Changes in time scale and sensitivity in the ommatidia of *Limulus. Journal of Physiology.* 172:239–263.

Green, D. G., J. E. Dowling, I. M. Siegel, and H. Ripps. 1975. Retinal mechanisms of visual adaptation in the skate. *Journal of General Physiology.* 65:483–502.

Green, D. G., and I. M. Siegel. 1975. Double branched flicker fusion curves from the all-rod skate retina. *Science.* 188:1120–1122.

Harosi, F. I. 1975. Absorption spectra and linear dichroism of some amphibian photoreceptors. *Journal of General Physiology.* 66:357–382.

Hecht, S., S. Shlaer, and M. H. Pirenne. 1942. Energy quanta, and vision. *Journal of General Physiology.* 25:819–840.

Lamb, T. D. 1984. Effects of temperature changes on toad photocurrents. *Journal of Physiology.* 346:557–578.

Lasater, E. M., J. E. Dowling, and H. Ripps. 1984. Pharmacological properties of isolated horizontal and bipolar cells from the skate retina. *Journal of Neuroscience.* 4:1966–1975.

Leibovic, K. N., J. E. Dowling, and Y. Y. Kim. 1987. Background and bleaching equivalence in steady-state adaptation of vertebrate rods. *Journal of Neuroscience.* 7:1056–1063.

Liebman, P. A., K. R. Parker, and E. A. Dratz. 1987. The molecular mechanism of visual excitation and its relation to the structure and composition of the rod outer segment. *Annual Review of Physiology.* 49:765–791.

Matthews, G. 1983. Physiological characteristics of single green rod photoreceptors from toad retina. *Journal of Physiology.* 342:347–359.

Naka, K.-I., R. L. Chappell, M. Sakuranaga, and H. Ripps. 1988. Dynamics of skate horizontal cells. *Journal of General Physiology.* 92:811–831.

Pepperberg, D. R., P. K. Brown, M. Lurie, and J. E. Dowling. 1978. Visual pigment and photoreceptor sensitivity in the isolated skate retina. *Journal of General Physiology.* 71:369–396.

Roof, D. J., and J. E. Heuser. 1982. Surfaces of rod photoreceptor disk membranes: integral membrane components. *Journal of Cell Biology.* 95:487–500.

Szamier, R. B., and H. Ripps. 1983. The visual cells of the skate retina: structure, histochemistry, and disc-shedding properties. *Journal of Comparative Neurology.* 215:51–62.